



Estimation of recruitment index of Pacific bluefin tuna based on real-time troll monitoring survey data using Vector Autoregressive Spatio-Temporal (VAST) model analysis

Ko Fujioka, Yohei Tsukahara, Saki Asai, Kirara Nishikawa,
Hiromu Fukuda and Shuya Nakatsuka

Highly Migratory Resources Division, Fisheries Resources Institute,
Japan Fisheries Research and Education Agency
5-7-1, Orido, Shimizu, Shizuoka 424-8633, JAPAN

December 2021

Working document submitted to the ISC Pacific bluefin tuna Working Group, International Scientific Committee for Tuna and Tuna-Like Species in the North Pacific Ocean (ISC), from 14 to 21 December 2021, Webinar.

Summary

In this document, we attempted to develop recruitment abundance indices (i.e. standardized CPUE) of age-0 Pacific bluefin tuna using data of real-time troll monitoring operated in the East China Sea during the winter season for two periods of 2011-2020 and 2017-2020 fishing year. The standardized CPUE was calculated by Vector Autoregressive Spatio-Temporal (VAST) model which a delta-generalized linear mixed model that separately formulates the encounter probability and the positive catch rate. Those estimated indices for each time period in this study were generally similar to the index based on the traditional sales slip data, which was used for the 2020 assessment. Furthermore, our candidate models complement the data-poor 2017 fishing year, in which operations were restricted due to a strict fishing regulation, thus the indices would be reasonable for input into the stock assessment model for the next assessment.

Introduction

The recruitment abundance index (i.e. standardized CPUE) is one of the most important input data for the Pacific bluefin tuna (PBF) stock assessment. This recruitment index (age-0) has been calculated using the sales slip data of the Japanese troll fishery operating in the East China Sea (ECS) during the winter season. However, while the sales slip data has an advantage of being available for a long period of time, there are several concerns due to the nature of source such as the lack of zero-catch data, rough spatial and temporal resolutions of samples (2 areas/date). In addition, Nishikawa et al. (2021) pointed out that recently introduced fishery management (catch allocation to each vessel (Individual Quota or Area based Quota)) has affected the number of operations, fishing season, operational purpose (for farming/market), and frequency of the live-release, while would not be captured by the sales slip data. Therefore, alternative information is necessary in order to correctly interpret the recent trends of recruitment.

As an alternative data source, the Fisheries Resource Institute in Japan has been conducting real-time troll monitoring survey since 2011 to collect catch and effort data with geographical information, which are transmitted to the institute in real-time through cellular networks (Tsukahara et al., 2019). Tsukahara et al. (2019) reported that those operational data with fine spatio-temporal resolution, which include live-release data and zero-catch operations, can be used to estimate standardized CPUE in a timely manner. Furthermore, the winter real-time monitoring survey maintains its consistency with

the sales slip CPUE in terms of the fishing season, fishing ground, and targeted age-0 PBF, which are born in two main spawning grounds (the North Western Pacific Ocean and the Sea of Japan). The performance of the estimated index using real-time monitoring data was reported as similar to traditional troll CPUE (Fukuda et al., 2021).

As a result of the review of recruitment index at the last PBF WG meeting, the WG recommended not to use traditional sales slip recruitment index after 2016, when negative bias may occur due to operation changes in response to strict management measures. Some members recommended the recruitment index based on real-time monitoring information as an alternative, but the WG preferred to discuss further in the coming data preparatory and assessment meetings.

The real-time troll monitoring data provides geographic information on operations by vessels, so allowing us to aggregate catch and effort into a detailed latitude-longitude grids. Applying to a spatio-temporal statistical model to those data is expected to have advantages such as an area-based weighting of samples, an accountability for variability in sampling over space, and those might provide a more accurate estimation of standardized CPUE. Recently, an attempt has been made to apply the Vector Autoregressive Spatio-Temporal (VAST) model to PBF of Taiwanese longline fishery data and compare with abundance indices from traditional GLMM models (Yuan et al. 2021).

In this study, we attempted to estimate recruitment indices for the entire data collection period from 2011 to 2020 and for the period of strict fishing regulations from 2017 to 2020, based on real-time troll monitoring data instead of sales slip data, which has been strongly affected by recent fishing regulations. We explored area-weighted recruitment index using the VAST approach, which spatio-temporal delta-generalized liner mixed modelling techniques (Thorson, 2019), with the hope of reducing bias due to decreased sampling area by fishing regulations. The results of those two periods (2011-2020 and 2017-2020 fishing year) are discussed and compared with indices calculated using the traditional results of the GLM (Nishikawa et al., 2021).

Methods

Data and data filtering

Data from 14 real-time troll monitoring vessels, which targeted for age-0 PBF (i.e. 40-60 cm fork length) during the winter season (November to following February) in the ECS were collected from 2011 to 2020 fishing year. These vessels equip the GPS receiver and numeric keypad to input number of fish caught at the fishing location. The GPS data is recorded at intervals of 1 second while all trips. The vessel velocity can be estimated by the moving distance based on the GPS data. The estimated

velocity was smoothed by the trimmed mean to exclude the obvious outlier due to the unsettled GPS data. These trace of fishing behavior and catch position enable to use more precise efforts in an operation, i.e., substantial operation time, than the catch per day used for sales slip data. PBF operation was defined as continuous vessel's velocity in the range of 2-7knot for more than 30 minutes. The PBF catch and effort (residence time in minutes) data were aggregated in a 0.1×0.1 degree latitude/longitude grids and formatted into the following data; vessel name, year, month, day, latitude, longitude, catch, effort.

For data filtering, the first step was to carefully review the aggregate data and use expert judges to remove any operations that were not clearly PBF operations based on the vessel's track and location records. This is because fishermen may operate targeting other fish species due to changes in the catchability of PBF and demand for farming depending on year and season. We also excluded two operations of data that had obvious errors in the numeric keypad entry on board (e.g., more than 500 catches in one operation). A total of 254 grids and 2,840 days of operational data by 14 vessels were obtained (for location, see Fig. 1 top). Second, data in the northeastern part of Tsushima (latitude >34.5, longitude >129.2) was excluded (38 grids) because it was a unique fishing ground only for the 2011 fishing year. This kind of data in rarely sampled area may affect the estimation of spatial effect of whole time series by the nature of VAST model for sharing information over space and time. Third, we filtered out the data in a grid where the amount of effort for each day and vessel was less than 5 minutes in an operation. It was determined that those short amounts of effort were just transit time of simply passing the edge of the 0.1 degree grid rather than the real operation time spent in that grid. Finally, we also filtered out the data where the numeric keypad was not entered at the exact catch location, such as when the keypad was entered after returning to their port. As a result of the data filtering described above, 213 grids (16% filter) and 2,801 days (1% filter) of data throughout the whole period 2011-2020 were used for the VAST analysis, as the distribution of operation is shown in the bottom of Figure 1.

As a summary of the data after filtering, a histogram of the fishing effort (in minutes) and the number of PBF caught for each data period is shown in Figure 2. In this 0.1 degree grids of aggregated data, the mean and standard deviation of fishing effort for 2011-2020 and 2017-2020 were 102.4 ± 104.7 and 129.6 ± 125.5 minutes, respectively, both ranging from 5 to 735 minutes. Also, the mean

and standard deviation of PBF catch in each period were 2.9 ± 9.9 and 3.6 ± 12.9 , respectively, with the same range of 0 to 265. Over the entire period (2011-2020), the operations of zero-catch rate was 69%, the positive catch rate was 31%, and the coefficient of variation of PBF catch was 3.41. The nominal CPUE for each month and each fishing year is shown in Figure 3.

Vector Autoregressive Spatio-Temporal (VAST) model

VAST is a delta-generalized linear mixed model that separately formulates the encounter probability and the positive catch rate, and is available from the R package “VAST” version 3.8.2 on the website (<https://github.com/James-Thorson-NOAA/VAST>) (Thorson, 2019). In our study, the encounter probability (p) at observation i was modeled using a logit-linked linear predictor, and the positive catch rate (r) at observation i was modeled using a log-linked linear predictor, as in the following equation:

$$(1) \text{logit}(p_i) = \beta_1(t_i) + L_{\omega_1}\omega_1(s_i) + L_{\varepsilon_1}\varepsilon_1(s_i, t_i) + \zeta_1(s_i, m_i) + L_{\eta_1}\eta_1(v_i)$$

$$(2) \log(r_i) = \beta_2(t_i) + L_{\omega_2}\omega_2(s_i) + L_{\varepsilon_2}\varepsilon_2(s_i, t_i) + \zeta_2(s_i, m_i) + L_{\eta_2}\eta_2(v_i)$$

where $\beta(t_i)$ is the intercept in year t_i , $\omega(s_i)$ is the time-invariant spatial variations at location s_i , $\varepsilon(s_i, t_i)$ is the time-varying spatio-temporal variations at location s_i in year t_i , $\zeta(s_i, m_i)$ is the s_i month effect m_i as a catchability covariate which is either spatially varying at location at s_i or spatially constant by configuration and $\eta(v_i)$ is the effect of vessel v_i as a factor of overdispersion, and L_{ω} , L_{ε} and L_{η} are the scaling coefficients of the random effect distributions.

The probability of the density c is specified in this study as follows for a zero-inflated Poisson distribution:

$$(3) \Pr(c_i = c) = \begin{cases} 1 - p_i & \text{if } c = 0 \\ p_i \times \text{ZeroInflated Poisson}(c_i | \log(r_i), \sigma^2) & \text{if } c > 0 \end{cases}$$

where σ^2 is a dispersion parameter.

Then, the abundance index was predicted using an area-weighted approach, which calculates total abundance as a weighted sum of the estimated densities in a pre-defined spatial domain of

knots. The number of knots was set equal to the number of observation locations (213 knots for 2011-2020 and 127 knots for 2017-2020).

Regarding the configuration of spatial structure with Gaussian Random Markov field (GRMR), this analysis used the anisotropic estimation of correlation, which estimate two different parameters for the correlation of two independent directions. In terms of temporal configuration, there is no assumption of correlated structure both year effect itself and spatio-temporal variation because the recruitment strength was highly varying over year based on the PBF assessment result.

Results and Discussion

In this study, area-weighted standardized CPUEs for two periods, 2011-2020 and 2017-2020, were estimated from spatio-temporal model analysis using real-time monitoring data (Fig. 7, left). For the 2011-2020 data period, the model (Case 1) that assumed spatial and spatio-temporal effects, month effect as catchability covariate which was spatially varying, and considered the vessel effect as an overdispersion factor for each of encounter probability and positive catch rate was judged to be the best model in terms of the AIC criteria (Table 1-1). On the other hand, for the 2017-2020 data, the model (Case 5) in which the month effect of encounter probability was adjusted to be spatially constant was determined to be the best (Table 1-2). The model converged successfully and the final gradients on each parameter were well below 1.36×10^{-7} for the 2011-2020 period (Table 2-1) and 1.06×10^{-7} for the recent period (Table 2-2). Quantile diagnostics of these models also showed no considerably negative signs in the standardization each data period (Fig. 8).

The result of distance of 10% correlation of both encounter probability and positive catch rate was estimated as anisotropic shapes with 45-60km of long axis mainly from south to north in each period of time (Fig. 5), so that the estimation in certain grids have some impacts on estimation in the approximately 3-4 grids away from there when 0.1 by 0.1 grid. This means spatial correlation seems to be limited for availability of age-0 PBF. Changes in the center of the PBF biomass in the east-west and north-south directions did not show a clear pattern with the estimated biomass (Fig. 6). For example, in the years when the estimated biomass was relatively high (Fig. 7, top left; 2013, 2016-2018), there was no specific density distribution trend in the Tsushima and Goto (north-south) or in

the east-west areas (Fig. 4). This may mean that the variation in the center of biomass occurs regardless of the strength of the recruitment and is not characteristic for long-term interannual variability.

The comparison of the standardized indices by VAST (Case 1 for 2011-2020 and Case 5 for 2017-2020) and traditional GLM index is shown in Figure 9. The indices estimated in this study were generally similar to the traditional ones throughout the period. As the results of operational changes responding to strict management measures, the recruitment index based on sales slip trend to negatively biased since 2016 (Nishikawa et al. 2021). Moderately high values in this real-time monitoring index after 2016 would likely reflect the difference of the data sources which include a live-release information only in a former one. In addition, the PBF of 2016 year class, which were caught as a notable peaks in various fishing gears/grounds, from size composition data, was confirmed as a relatively dominant year class (e.g., Tsukahara et al., 2021). Therefore, the index for 2016 estimated from this study would be reasonable. The index has a relative large standard errors in 2017 (Fig. 7), possibly due to limited data not only for seasonal coverage but also spatial coverage by fishing regulations (fishery ban in the latter half of 2017 fishing year). This means the estimation in 2017 includes many expectations with spatial correlation structure but without data. Although the estimated value in 2017 is still point of contention as well as a traditional CPUE, the recruitment abundance indices in this study are considered reasonable and can be a candidate for the use in the stock analysis.

References

- Fukuda, H., Fujioka, K., Tsukahara, Y., Nishikawa, K. and Nakatsuka, S. 2021. Reinforcement of Japanese PBF recruitment monitoring program. ISC/21/PBFWG-1/06.
- Nishikawa, K., Tsukahara, Y., Fujioka, K., Fukuda, H. and Nakatsuka, S. 2021. Update of age-0 PBF index based on catch per unit effort data from Japanese troll fishery and its associated issues. ISC/21/PFWG-1/05.
- Thorson, JT. 2019. Guidance for decisions using the Vector Autoregressive Spatio-Temporal (VAST) package in stock, ecosystem, habitat and climate assessments. *Fish. Res.* 210: 143-161.
- Tsukahara, Y. and Chiba, K. 2019. Real-time recruitment monitoring for Pacific bluefin tuna using

CPUE for troll vessels: Update up to 2018 fishing year. ISC/19/PBFWG-1/04.

Tsukahara, Y., Fukuda, H. and Nakatsuka, S. 2021. Update of standardized CPUE and catch at size for Pacific bluefin tuna (*Thunnus orientalis*) caught by Japanese coastal and offshore longline up until 2019 fishing year. ISC/21/PBFWG-1/04.

Yuan, TL., Chang, SK., Liu, HI. and Huang, CC. 2021. Size pattern and relative CPUE of Taiwanese PBF fisheries using delta-generalized liner mixed models (GLMM) and vector-auto-regressive spatio-temporal model (VAST). ISC/21/PBFWG-1/03.

Table 1-1 For the period 2011-2020, combinations of explanatory variables for encounter probability (p) and positive catch (r) in a delta model and the values of Akaike information criterion (AIC). Delta AIC indicates the difference between the case 1 model with the lowest AIC.

Case	Model for p	Model for r	AIC	Δ AIC
1	Yr + Station + Yr:Station + Month(spatially varying) + Vessel	Yr + Station + Yr:Station + Month(spatially varying) + Vessel	42851	0
2	Yr + Station + Yr:Station + Month(spatially varying)	Yr + Station + Yr:Station + Month(spatially varying)	43584	733
3	Yr + Station + Yr:Station + Month(spatially constant)	Yr + Station + Yr:Station + Month(spatially varying)	43595	744
4	Yr + Station + Yr:Station + Month(spatially varying)	Yr + Station + Yr:Station + Month(spatially constant)	45006	2155
5	Yr + Station + Yr:Station + Month(spatially constant)	Yr + Station + Yr:Station + Month(spatially constant)	45040	2189
6	Yr + Yr:Station + Month(spatially varying)	Yr + Station + Yr:Station + Month(spatially varying)	43674	823
7	Yr + Station + Month(spatially varying)	Yr + Station + Yr:Station + Month(spatially varying)	43769	918

Table 1-2 Continuing with the dataset for the period 2017-2020. Delta AIC indicates the difference between the case 5 model with the lowest AIC.

Case	Model for p	Model for r	AIC	Δ AIC
1	Yr + Station + Yr:Station + Month(spatially varying) + Vessel	Yr + Station + Yr:Station + Month(spatially varying) + Vessel		
2	Yr + Station + Yr:Station + Month(spatially varying)	Yr + Station + Yr:Station + Month(spatially varying)		
3	Yr + Station + Yr:Station + Month(spatially constant) + Vessel	Yr + Station + Yr:Station + Month(spatially constant) + Vessel	17589	833
4	Yr + Station + Yr:Station + Month(spatially constant)	Yr + Station + Yr:Station + Month(spatially constant)	17919	1163
5	Yr + Station + Yr:Station + Month(spatially constant) + Vessel	Yr + Station + Yr:Station + Month(spatially varying) + Vessel	16756	0
6	Yr + Station + Yr:Station + Month(spatially constant)	Yr + Station + Yr:Station + Month(spatially varying)	17136	380
7	Yr + Station + Yr:Station + Month(spatially varying) + Vessel	Yr + Station + Yr:Station + Month(spatially constant) + Vessel	17528	772
8	Yr + Station + Yr:Station + Month(spatially varying)	Yr + Station + Yr:Station + Month(spatially constant)	17859	1103

Table 2-1 Initial and final condition of each parameter related to explanatory variables in the 2011-2020 period. The list of parameters is as follows:

beta; intercept for 1st or 2nd linear predictor (1st; encounter probability, 2nd; positive catch rate) each fishing year (2011-2020)

L_eta; overdispersion factors (vessels) for 1st or 2nd linear predictor

L_omega; spatial factors for 1st or 2nd linear predictor

L_epsilon; spatio-temporal factors for 1st or 2nd linear predictor

logkappa; decorrelation rate for 1st or 2nd linear predictor

log_sigmaPh; conditional variance between each month for intercepts of 1st linear predictor

Parameter	Starting value	Lower boundary	Maximum likelihood estimation	Upper boundary	Final gradient
ln_H_input	-0.192	-5	-0.192	5	-5.47E-09
ln_H_input	-0.076	-5	-0.076	5	-1.71E-09
beta1_ft_2011	-0.520	-Inf	-0.520	Inf	8.52E-10
beta1_ft_2012	-0.903	-Inf	-0.903	Inf	1.11E-09
beta1_ft_2013	-0.414	-Inf	-0.414	Inf	2.04E-09
beta1_ft_2014	-1.011	-Inf	-1.011	Inf	1.35E-09
beta1_ft_2015	-0.591	-Inf	-0.591	Inf	8.87E-10
beta1_ft_2016	0.383	-Inf	0.383	Inf	6.75E-10
beta1_ft_2017	0.645	-Inf	0.645	Inf	-8.25E-10
beta1_ft_2018	-0.340	-Inf	-0.340	Inf	7.62E-10
beta1_ft_2019	-0.899	-Inf	-0.898	Inf	5.30E-10
beta1_ft_2020	-0.600	-Inf	-0.600	Inf	-6.33E-11
L_eta1_z	0.824	-Inf	0.824	Inf	-1.14E-07
L_omega1_z	-1.014	-Inf	-1.014	Inf	1.36E-07
L_epsilon1_z	0.744	-Inf	0.744	Inf	-2.29E-08
logkappa1	-2.815	-4.790245	-2.815	-1.173742	1.31E-07
log_sigmaPhi1_k	-0.832	-Inf	-0.832	Inf	-3.87E-09
log_sigmaPhi1_k	-1.286	-Inf	-1.287	Inf	1.72E-08
log_sigmaPhi1_k	-0.127	-Inf	-0.127	Inf	-3.93E-09
beta2_ft_2011	-3.383	-Inf	-3.383	Inf	1.22E-09
beta2_ft_2012	-3.413	-Inf	-3.413	Inf	-5.99E-09
beta2_ft_2013	-3.008	-Inf	-3.008	Inf	1.77E-09
beta2_ft_2014	-4.217	-Inf	-4.217	Inf	7.21E-09
beta2_ft_2015	-3.929	-Inf	-3.929	Inf	4.95E-09
beta2_ft_2016	-3.037	-Inf	-3.037	Inf	-4.52E-09
beta2_ft_2017	-2.952	-Inf	-2.952	Inf	1.94E-09
beta2_ft_2018	-2.890	-Inf	-2.890	Inf	-5.42E-09
beta2_ft_2019	-3.576	-Inf	-3.576	Inf	1.10E-09
beta2_ft_2020	-3.450	-Inf	-3.450	Inf	1.61E-09
L_eta2_z	-0.235	-Inf	-0.235	Inf	-8.18E-10
L_omega2_z	-0.125	-Inf	-0.125	Inf	2.17E-09
L_epsilon2_z	-0.836	-Inf	-0.836	Inf	6.29E-08
logkappa2	-2.053	-4.790245	-2.053	-1.173742	1.45E-08
log_sigmaPhi2_k	-0.329	-Inf	-0.329	Inf	2.67E-10
log_sigmaPhi2_k	-0.452	-Inf	-0.452	Inf	-4.08E-09
log_sigmaPhi2_k	-0.548	-Inf	-0.548	Inf	-3.54E-09

Table 2-2 Continuing with the dataset for the period 2017-2020.

Parameter	Starting value	Lower boundary	Maximum likelihood estimation	Upper boundary	Final gradient
ln_H_input	-0.264	-5	-0.264	5	-1.06E-07
ln_H_input	-0.048	-5	-0.048	5	-4.14E-08
beta1_ft_2017	-0.051	-Inf	-0.051	Inf	-1.12E-09
beta1_ft_2018	-0.687	-Inf	-0.687	Inf	1.86E-08
beta1_ft_2019	-1.513	-Inf	-1.513	Inf	1.60E-09
beta1_ft_2020	-1.169	-Inf	-1.169	Inf	-5.40E-09
lambda1_k	0.194	-Inf	0.194	Inf	-7.95E-09
lambda1_k	0.592	-Inf	0.592	Inf	2.81E-08
lambda1_k	0.954	-Inf	0.954	Inf	-1.91E-08
L_eta1_z	1.058	-Inf	1.058	Inf	-1.41E-08
L_omega1_z	-1.019	-Inf	-1.019	Inf	6.20E-08
L_epsilon1_z	-0.841	-Inf	-0.841	Inf	3.52E-08
logkappa1	-2.534	-4.733377	-2.534	-1.176148	-1.55E-08
beta2_ft_2017	-2.947	-Inf	-2.947	Inf	1.33E-09
beta2_ft_2018	-2.694	-Inf	-2.694	Inf	3.08E-10
beta2_ft_2019	-3.672	-Inf	-3.672	Inf	5.42E-09
beta2_ft_2020	-3.564	-Inf	-3.564	Inf	2.38E-09
L_eta2_z	-0.349	-Inf	-0.349	Inf	1.83E-08
L_omega2_z	0.000	-Inf	0.000	Inf	-2.56E-09
L_epsilon2_z	1.021	-Inf	1.021	Inf	-6.86E-08
logkappa2	-2.240	-4.733377	-2.240	-1.176148	1.18E-08
log_sigmaPhi2_k	-0.358	-Inf	-0.358	Inf	-9.36E-09
log_sigmaPhi2_k	0.184	-Inf	0.184	Inf	2.79E-08
log_sigmaPhi2_k	-0.222	-Inf	-0.222	Inf	-1.06E-08

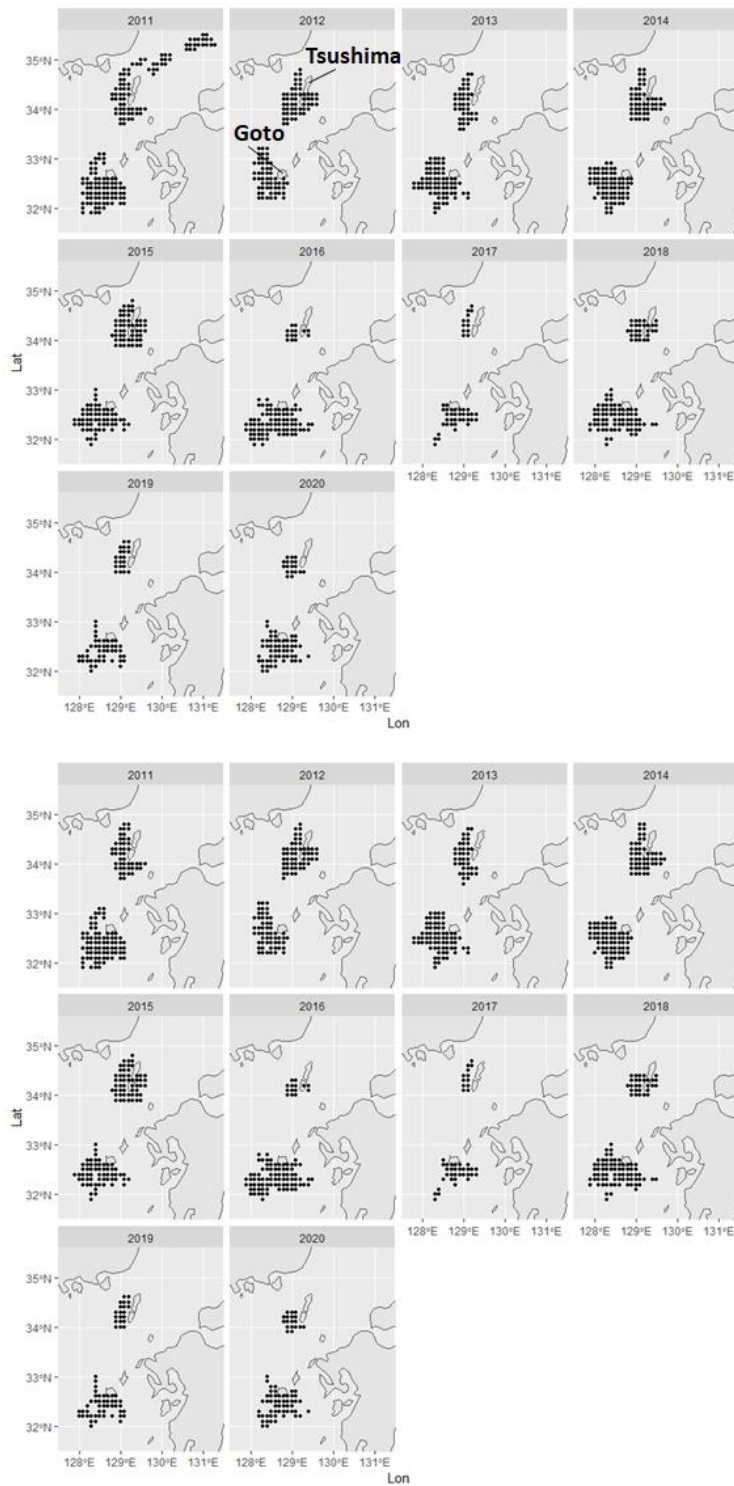


Figure 1 Distribution of troll operations of 14 real-time monitoring vessels from 2011 to 2020 fishing year is shown in the raw data (top) and after filtering (bottom). The post-filtered data are used for

abundance estimation by the VAST model analysis.

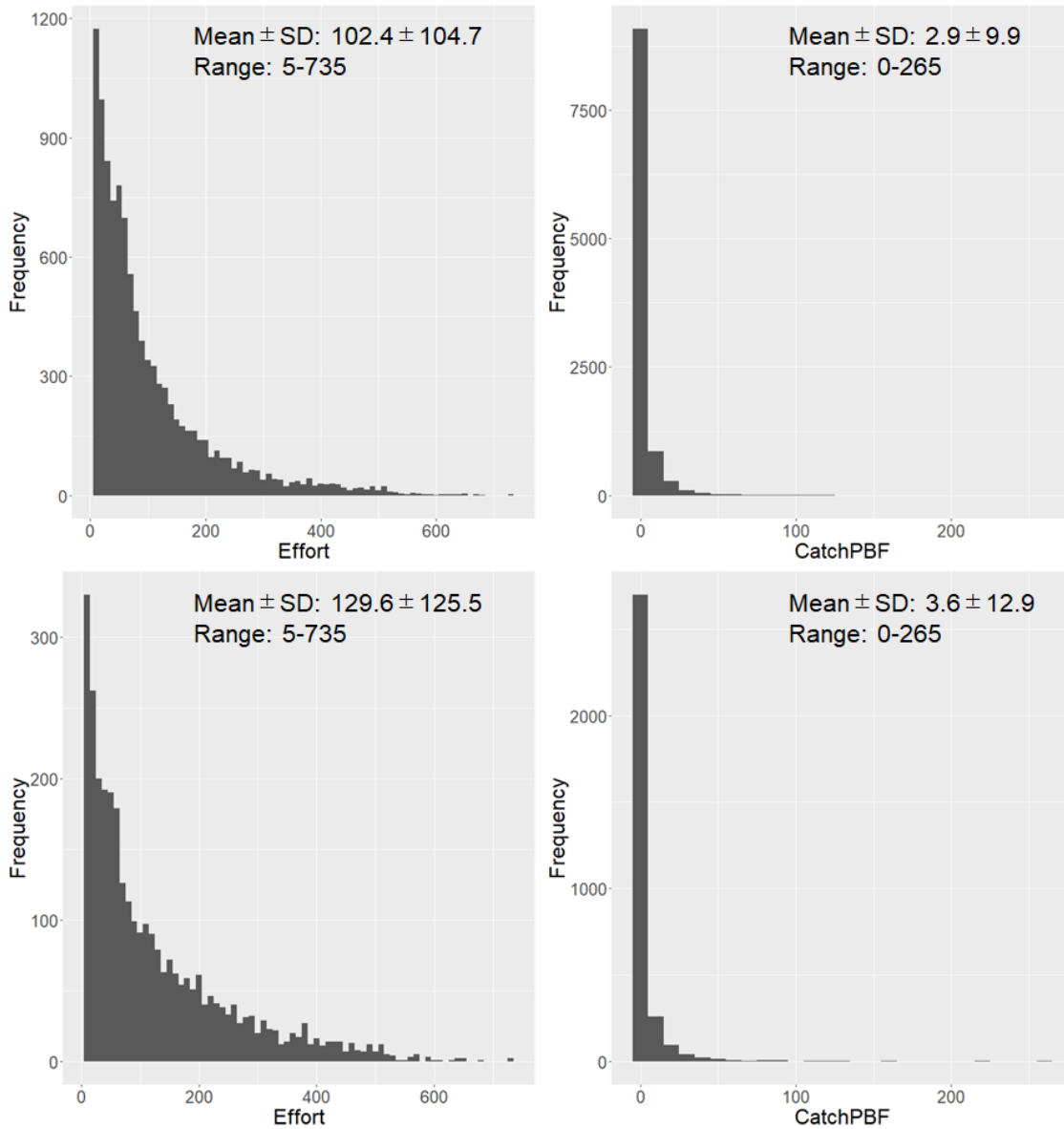


Figure 2 Frequency of fishing efforts (left) and PBF catches (right) for the two periods 2011-2020 (top) and 2017-2020 (bottom) based on 0.1 degree grid aggregate data.



Figure 3 Nominal CPUE during 2011-2020 fishing year for each month (November to following February). No operations during the months of January and February of 2017 due to fishing regulations.

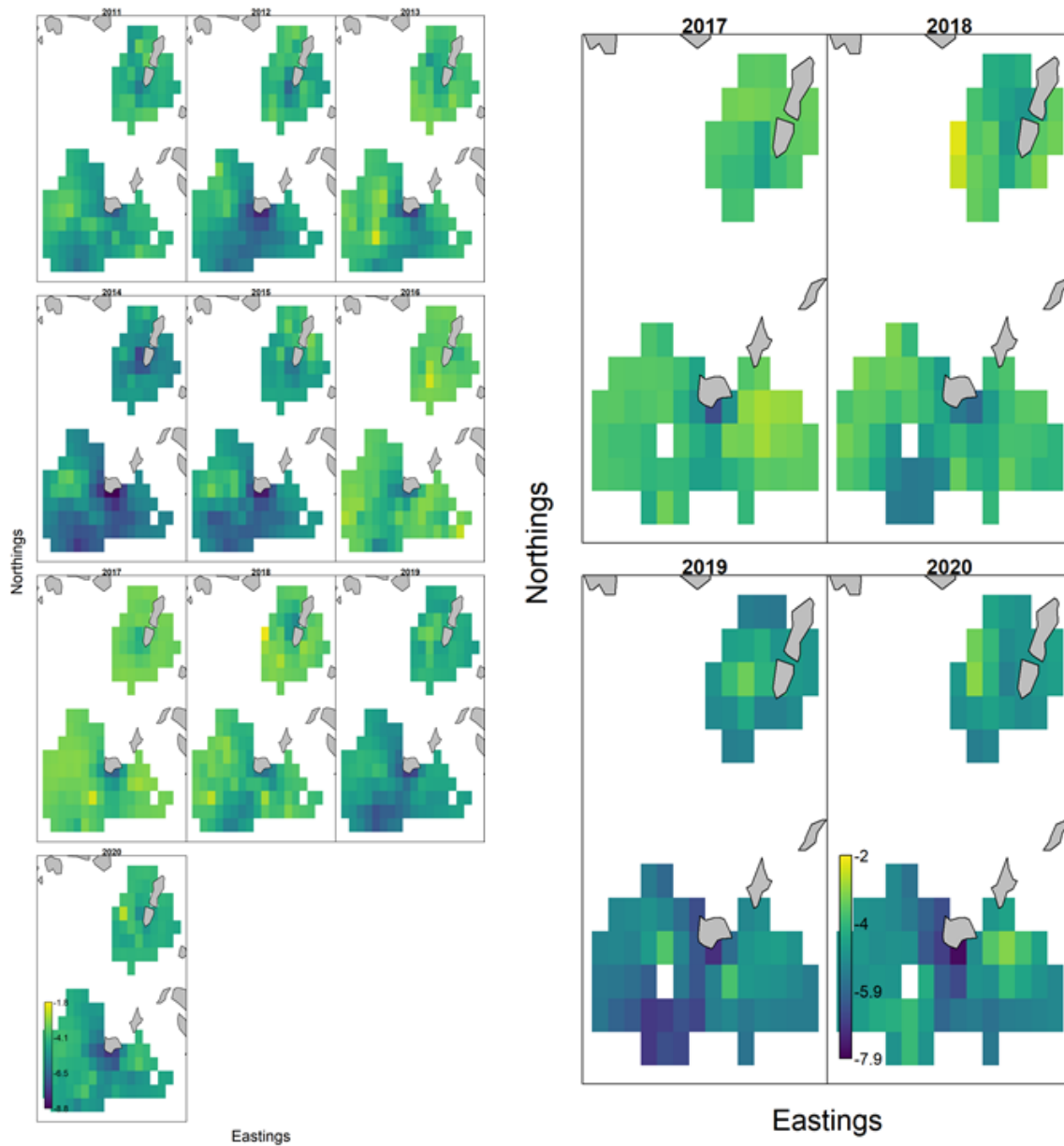


Figure 4 Spatio-temporal distribution of the log-transformed predicted densities of PBF for the 2011-2020 (left) and 2017-2020 (right) fishing year analyzed by VAST model. Warmer and cooler colors indicate high and low values, respectively.

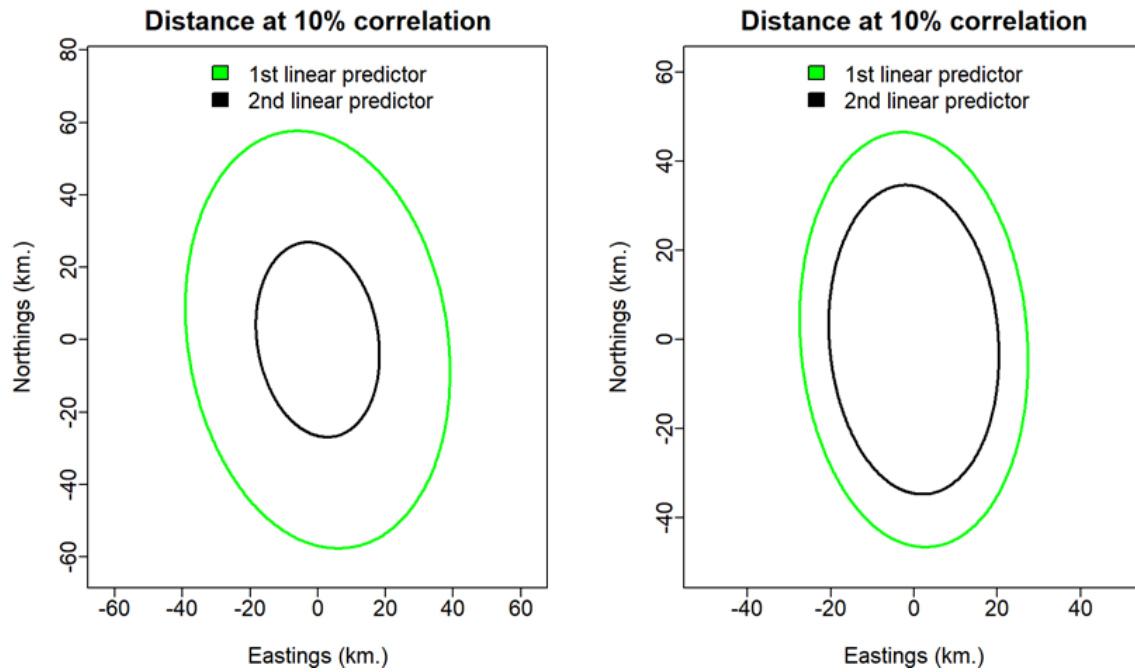


Figure 5 Decorrelation distance for different directions relative to encounter probability and positive catch rate for each of the two data periods 2011-2020 (left) and 2017-2020 (right). Indicating the magnitude of 2-dimensional spatial autocorrelation, and the ellipse signifies the distance (from a point located at position (0,0)), where the correlation drops to 10 %. The predicted densities correlated over a longer distance in the north-south direction than in the east-west direction.

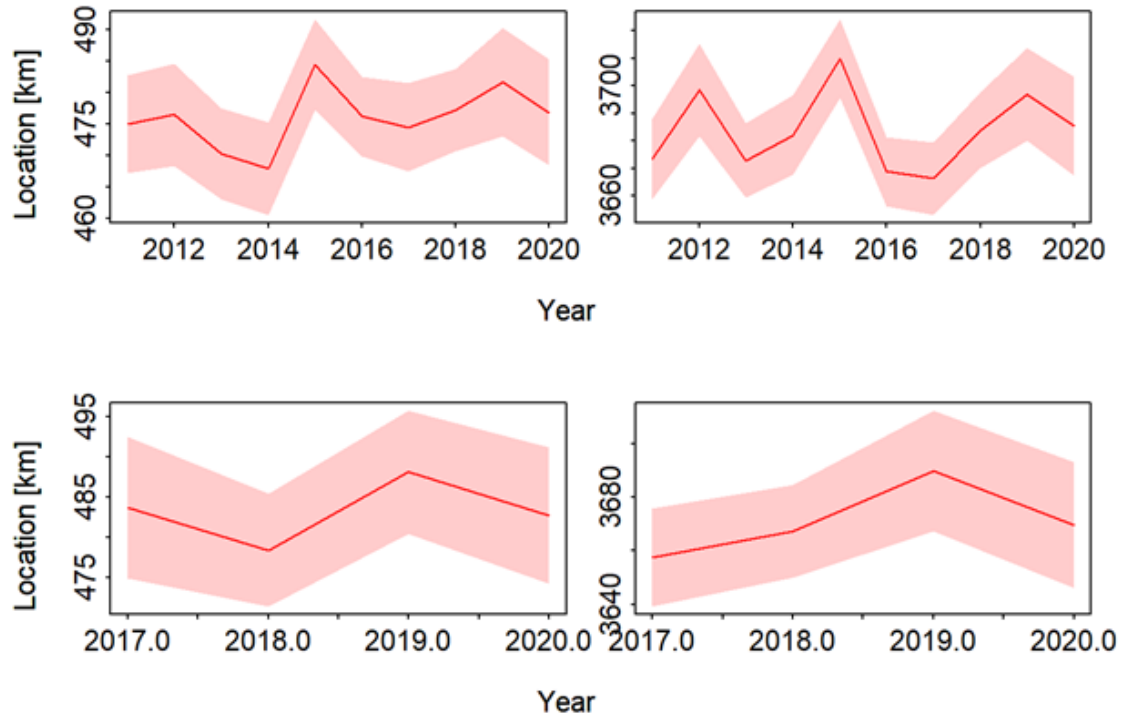


Figure 6 The center of gravity of PBF recruitments indicating the shift in distribution (distance (km)) in the east-west (left) and north-south (right) directions for the periods 2011-2020 (top) and 2017-2020 (bottom). The thick line with shading indicates the mean value and standard error.

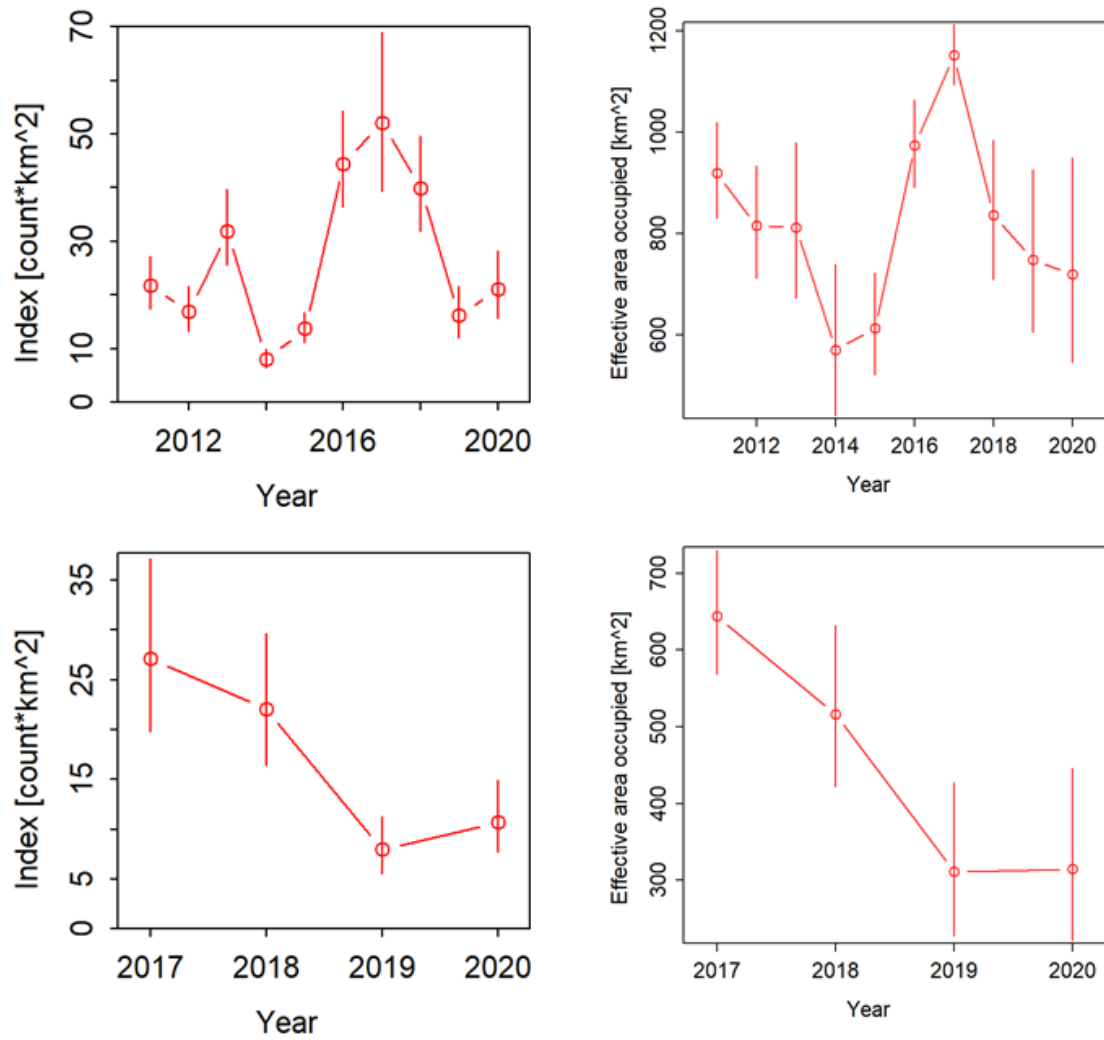


Figure 7 Standardized index of relative abundance of PBF (left) and estimated of the effective area occupied by PBF indicating range expansion/contraction (right) for the periods 2011-2020 (top) and 2017-2020 (bottom). The open circles with vertical lines denote point estimates with standard errors.

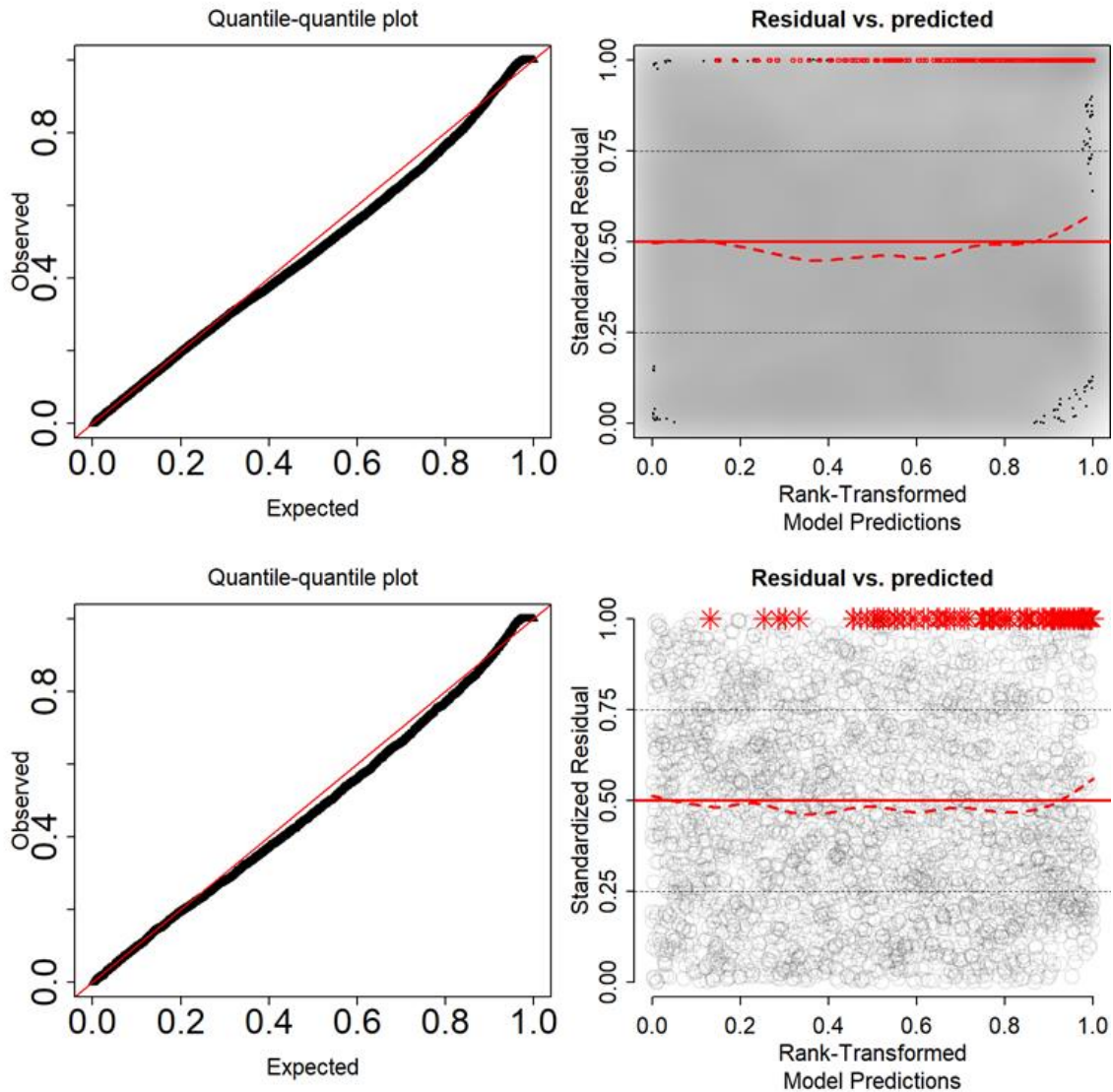


Figure 8 Diagnostic Q-Q plot (left) and residual plots (right) comparing the observed and predicted quantiles for the periods 2011-2020 (top) and 2017-2020 (bottom). The residual plot calculating a quantile regression to compare the empirical 0.5 quantile in y-direction (dashed red lines) with the theoretical 0.5 quantile (red solid line).

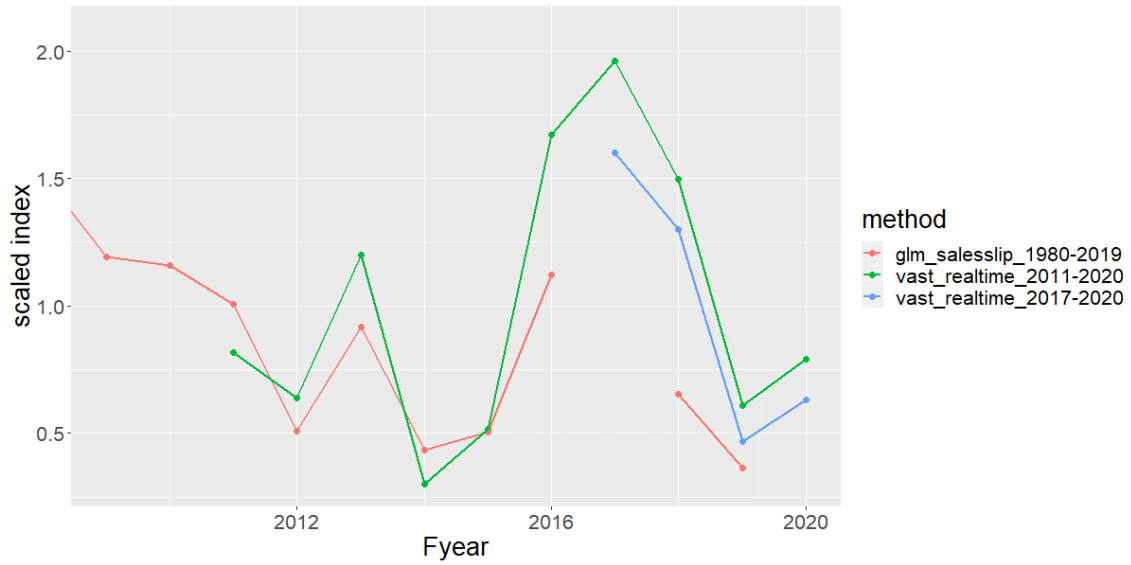


Figure 9 Recent trends of scaled abundance indices on results both traditional GLM (red line) using sales slip data (Nishikawa et al. 2021) and VAST analyses for the periods 2011-2020 (green line) and 2017-2020 (blue line) using real-time monitoring data (this study).